[CANCER RESEARCH 64, 6041–6049, September 1, 2004]

The *Rgr* Oncogene Induces Tumorigenesis in Transgenic Mice

María Jiménez,[1,2] Ignacio Pérez de Castro,[1,2] Marta Benet,[1] Juan F. García,[2] Giorgio Inghirami,[1,3] and Angel Pellicer[1]

[1]Department of Pathology and New York University Cancer Institute, New York University School of Medicine, New York, New York; [2]Molecular Pathology and Molecular Oncology Program, Centro Nacional de Investigaciones Oncológicas, Madrid, Spain; and [3]Center for Experimental Research and Medical Studies, University of Turin, Turin, Italy

ABSTRACT

To study the oncogenic potential of Rgr *in vivo*, we have generated several transgenic *Rgr* mouse lines, which express the oncogene under the control of different promoters. These studies revealed that *Rgr* expression leads to the generation of various pathological alterations, including fibrosarcomas, when its transgenic expression is restricted to nonlymphoid tissues. Moreover, the overall incidence and latency of fibrosarcomas were substantially increased and shortened, respectively, in a $p15^{INK4b}$-defective background. More importantly, we also have demonstrated that *Rgr* expression in thymocytes of transgenic mice induces severe alterations in the development of the thymocytes, which eventually lead to a high incidence of thymic lymphomas. This study demonstrates that oncogenic Rgr can induce expression of $p15^{INK4b}$ and, more importantly, that both Rgr and $p15^{INK4b}$ cooperate in the malignant phenotype *in vivo*. These findings provide new insights into the tumorigenic role of *Rgr* as a potent oncogene and show that $p15^{INK4b}$ can act as a tumor suppressor gene.

INTRODUCTION

Rgr is an oncogene that was isolated in our laboratory by its ability to produce tumors in the nude mice assay (1). This oncogene was detected and isolated by gene transfer, using DNA from a 7,12-dimethylbenz(*a*)anthracene-induced rabbit squamous cell carcinoma as the starting material. *Rgr* (truncated at its 5′ end) was fused to the *rHHR23A* gene, the rabbit orthologue of *Rad23*, a *Saccharomyces cerevisiae* nucleotide excision repair gene. Rgr belongs to the guanine nucleotide exchange factor (GEF) family, also known as GDP dissociation stimulator (GDS), and has a significant homology to Ral guanine dissociation stimulator (Ral-GDS). Ral-GDS is an effector of Ras and may functionally link Ras with other Ras-related proteins (2). Similar to Ral-GDS, Rgr has been shown to have specific exchange activity for Ral (1). Rgr lacks the Ras-interacting domain within the COOH-terminal end present in other family members. Interestingly, its introduction into cells resulted in increased levels of GTP-bound Ras (3). Moreover, *Rgr* is the first member of the Ral-mediated pathway to display tumorigenic properties as demonstrated by the potent tumorigenic activity of *Rgr* in the nude mice assay (1) and the formation of transformed foci and abnormal cellular morphologies in cultured cells (3). In addition, Rgr also enhanced the phosphorylation of extracellular signal-regulated kinases, p38, and c-Jun-NH_2-terminal kinases. The biological significance of these activities was confirmed using dominant-negative forms of Ras, Ral, and Rho that blocked the transcriptional activation induced by Rgr (3). Interestingly, only the dominant-negative form of Ras inhibited Rgr transformation, indicating that Ras activation is crucial for the oncogenic activity of Rgr (3).

It is important to note that Ras has been previously shown to induce the expression of several cell cycle regulators, including $p15^{INK4b}$ (4), and it is important to determine the ability of Rgr to produce those effects. In addition, it has been previously shown that there is Ras activation and inactivation of $p15^{INK4b}$ in some tumors (5). This seemingly contradictory observation is interpreted as if the increase in $p15^{INK4b}$ expression produced by Ras is a defense mechanism of the cell to block the transforming effects of Ras. Therefore, it is also of interest to investigate whether Rgr would cooperate with $p15^{INK4b}$ inactivation as well.

Recently, we have shown that at least part of the transforming activity of *Rgr* is a consequence of its overexpression, which in turn is due to the elimination of translational regulatory elements in the 5′ leader region of *Rgr* mRNA. This overexpression resulted in subsequent Ras activation (6). The human orthologue of the rabbit *Rgr* gene, *hrgr*, has been recently isolated from lymphoid malignant cell lines that express several hrgr mutant transcripts (7). Similar to the activated rabbit truncated form (Rgr oncogene), the human mutant transcripts found in T-cell lines and some T-cell lymphomas are truncated forms of the *hrgr* gene (7).

This report summarizes the analysis of *Rgr* transgenic mouse lines in an effort to study the *in vivo* oncogenic potential of Rgr. In these experiments, Rgr has demonstrated the ability to induce pathological alterations, including tumors, in tissues in which it is expressed. Some of the neoplasic alterations were substantially increased in a $p15^{INK4b}$-defective background, indicating cooperation between these two genetic alterations in some tumor types for Rgr-induced tumorigenesis. More importantly, the expression of Rgr in T cells was able to cause the formation of lymphomas with a high penetrance, consistent with the alteration found in human lymphomas and confirming the important role of this oncogene in this type of tumor.

MATERIALS AND METHODS

Plasmids and DNA/RNA Manipulation. *Rgr* was subcloned into the *Eco*RI site of pcDNA3 vector (Invitrogen, Carlsbad, CA), in which the mCC10 promoter was put in place of the cytomegalovirus (CMV) promoter, giving rise to the pmCC10-RGR plasmid; or into pCX vector (8), giving rise to the pCX-RGR plasmid. *Rgr* also was subcloned into pMexNeo expression vector (9), producing pNM11 plasmid, which was described previously (3). The pCD4-RGR-Flag vector, in which the CD4 promoter drives RGR-Flag expression, was prepared by inserting the CD4 promoter-enhancer into the cloning site of pMexNeo vector and then subcloning the RGR-Flag sequence in the 3′ end of the promoter. The CD4 promoter-enhancer was obtained from a plasmid (CD4-hCD2; a generous gift from Dr. D. R. Littman; Skirball Institute, New York University Medical Center, New York, NY) containing the minimal CD4 enhancer (339 bp), the minimal murine CD4 promoter (487 bp lacking the CD4 silencer region to drive the expression in CD4- and CD8-positive T cells, both single and double positive), the transcription initiation site, and 70 bp of the untranslated first exon and part of the first intron of the murine CD4 gene (10). The RGR-Flag fragment was described previously as Flag-tagged RSC-Rgr (6).

The expression of oncogenic *Rgr* driven by the majority of the promoters listed above was analyzed *in vitro* before obtaining the transgenic mice. pNM11 and pCX-RGR vectors were transfected into NIH3T3 cells by the calcium phosphate precipitation method (11), and the expression of Rgr was

Received 10/28/03; revised 5/16/04; accepted 7/6/04.

Grant support: Supported by National Institutes of Health grants CA50434 (A. Pellicer) and CA90773 (G. Inghirami).

The costs of publication of this article were defrayed in part by the payment of page charges. This article must therefore be hereby marked *advertisement* in accordance with 18 U.S.C. Section 1734 solely to indicate this fact.

Requests for reprints: Angel Pellicer, Department of Pathology and New York University Cancer Institute, New York University School of Medicine, 550 First Avenue, New York, NY 10016. Phone: 212-263-5342; Fax: 212-263-8211; E-mail: pellia01@med.nyu.edu.

tested using a focus formation assay and Northern blot. The expression of RGR in pmCC10-RGR vector was confirmed by transfecting H441 lung cells by the calcium phosphate precipitation method and performing a Northern blot. In addition, the luciferase reporter plasmids ($p15^{INK4b}$ promoter) used in this work were described previously (4).

For hybridizations, digested DNA or RNA was separated on agarose gels and transferred onto nitrocellulose membranes (Schleicher & Schuell, Keene, NH). DNA probes were labeled with [^{32}P]dCTP (3,000 Ci/mmol; Dupont-New England Nuclear, Boston, MA) using the Random Prime DNA Labeling System Rediprime II (Amersham Biosciences, Piscataway, NJ) in accordance with the manufacturer's protocol. Hybridizations were visualized by the use of a PhosphorImager (Molecular Dynamics, Sunnyvale, CA) or by exposure to X-ray film.

Generation and Genotyping of Transgenic Mice. Transgenic mice were generated as described previously (12, 13). Briefly, each of the transgene constructs was injected into the pronucleus of fertilized eggs from female donors and subsequently transferred to pseudopregnant mice. All of the transgenic lines were produced in the inbred strain FVB/N (14). Screening of positive animals for the transgene was performed by polymerase chain reaction (PCR) of DNA extracted as described previously (15), using forward primers specific for each of the promoters and the common reverse primer 907–884 (5′-GTGCCTGGCTGCAGGCTCCGCAGG-3′), which is specific for the transgene. The specific primers for each of the promoters were as follows: MSV-F (5′-ACCTGAAAATGACCCTGTGC-3′) for the MSV-RGR lines; mCC10-147 (5′-GGTCCTCCACTGCCTGAATA-3′) for the mCC10-RGR lines; PCX-F1 (5′-CAGCCATTGCCTTTTATGGT-3′) for the CMV-RGR lines; and CD4-RGR-F1 (5′-GCCCACTTTTGGGTATCAGA-3′) for the CD4-RGR-Flag lines. Founder animals were confirmed by Southern blot after digestion of 20 μg of genomic DNA with *Sac*I and hybridization with a cDNA probe containing the entire sequence of oncogenic rabbit Rgr. Screening of the offspring was performed by PCR amplification of DNA with the primers described above. The animals were maintained in accordance with National Institutes of Health and New York University institutional guidelines in a pathogen-free facility.

KO-$p15^{INK4b}$ mice were generously provided by M. Barbacid (Spanish National Cancer Institute, Madrid, Spain) in a 129/Sv × C57BL6 genetic background. MSV-RGR/$p15^{+/-}$ offspring were generated as littermates from common matings and genotyped by PCR using specific primers for the RGR transgene and both the wild-type and KO $p15^{INK4b}$ sequences (15). The MSV-RGR/$p15^{INK4b}-/-$ line was generated by crossing MSV-RGR/$p15^{INK4b}+/-$ mice and then maintained by mating the double mutants, MSV-RGRp15−/−.

Cell Culture and Luciferase Assays. NIH3T3 cells were maintained in Dulbecco's modified Eagle's medium (Invitrogen) supplemented with 10% calf serum (Invitrogen), penicillin G (50 units/ml), streptomycin (50 μg/ml; Gemini Bio-Products, Woodland, CA), and 500 μg/ml fungizone (Invitrogen) and incubated in standard conditions of humidity (95%), CO_2 atmosphere (5%), and temperature (37°C).

For the luciferase assays, approximately 75 ng of the reporter plasmids, 25 ng of the pRL-null (as an internal control of transfection efficiency), and 400 ng of the inducer (pNM11) or empty vector (pMEXneo) were used to cotransfect NIH3T3 cells. Transient transfections were performed by lipofection following the manufacturer's recommendations. NIH3T3 cells were plated onto 6-well plates (NIH3T3) at a density of 100,000 cells/well, grown for 24 hours, and transfected. Forty-eight hours after transfection, cells were collected, and the luciferase assay was performed in accordance with the manufacturer's recommendations (Dual-Luciferase Reporter Assay System; Promega, Madison, WI).

Real-Time Reverse Transcription-PCR Expression Analysis. Total RNA was isolated from tissues and cells using Trizol (Invitrogen). To generate cDNA, 1 μg of total RNA was reverse transcribed using 0.4 μmol/L of an oligo(dT)-adapter primer and SuperScript II RNase H reverse transcriptase (Invitrogen) as described by manufacturer. To determine $p15^{INK4b}$ mRNA expression in thymic lymphomas and wild-type thymi, real-time reverse transcription (RT)-PCR was performed using the following primers for mouse $p15^{INK4b}$: E2mp15F74, 5′-CTGCCACCCTTACCAGACCTGTGC-3′; and E2mp15R257, 5′-TCTCCAGTGGCAGCGTGCAGATAC-3′. To normalize the expression levels of p15, β-actin expression was also determined using primers QmBactin-F (5′-TGTTACCAACTGGGACGACA-3′) and QmBactin-R (5′-CTTTTCACGGTTGGCCTTAG-3′). Quantitative PCR was performed with the iCycler iQ System from Bio-Rad (Hercules, CA) using SYBR Green as DNA intercalator.

Histological and Immunohistochemical Analyses. Tissues were fixed in 10% buffered formalin at 4°C overnight, transferred to 70% ethanol, embedded in paraffin, and sectioned at 5-μm thickness. Sections were stained with hematoxylin and eosin for histological analysis.

The immunohistochemical expression of lineage-specific markers for B cells and IgM was performed on paraffin-embedded tissue sections from MSV-RGR/KO-$p15^{INK4b}$ and CD4-RGR lymphomas (spleen and thymus, respectively). Antibodies used were CD45R (goat antimouse B220; clone RA3-6B2; PharMingen, San Diego, CA) and rabbit antimouse IgM (DAKO, Glostrup, Denmark), respectively. A previous heat-induced epitope retrieval step was performed in a 0.1 mol/L trisodium citrate solution for 2 minutes in a conventional pressure cooker. After incubation, immunodetection was performed with the proper biotinylated secondary immunoglobulins, followed by peroxidase-labeled streptavidin (DAKO). Diaminobenzidine was used as substrate chromogen.

Immunostaining techniques were also performed in paraffin-embedded tissue sections for the detection of p53, p21, and p16 as described above. Antibodies used were as follows: rabbit antimouse p16 (M-156; 1:35 dilution; Santa Cruz Biotechnology, Santa Cruz, CA), rabbit antimouse p21 (C-19; 1:25 dilution; Santa Cruz Biotechnology), and rabbit antimouse p53 (CM5p; 1:100 dilution; Novocastra, Newcastle upon Tyne, United Kingdom).

Flow Cytometric Analysis. Primary thymocytes (0.5×10^6 per point) were isolated from 6-week-old wild-type and CD4-RGR mice. To characterize the different thymocyte subpopulations as well as their activation status, CD3, CD4, CD8, CD25, CD44, and CD69 markers were detected in both groups of thymocytes. Briefly, isolated thymocytes were washed twice with PBS and incubated at 4°C for 1 hour with two different sets of antibodies from CALTAG: PE-TexasRed-antiCD8, FITC-antiCD4, PE-antiCD44, and APC-antiCD25; or FITC-antiCD3 plus PE-antiCD69. Cells were washed three times with PBS and fixed with 2% paraformaldehyde. Finally, cells were analyzed by flow cytometry in a FACscan cytometer, and data were interpreted using the CellQuest program (Becton Dickinson, San Jose, CA).

RESULTS

Study of the Effect of *Rgr* Transgene Expression in Nonlymphoid Mouse Tissues. To determine whether the oncogenic form of Rgr is able to elicit the formation of tumors *in vivo*, we have inserted its cDNA into transgene cassettes to generate different transgenic

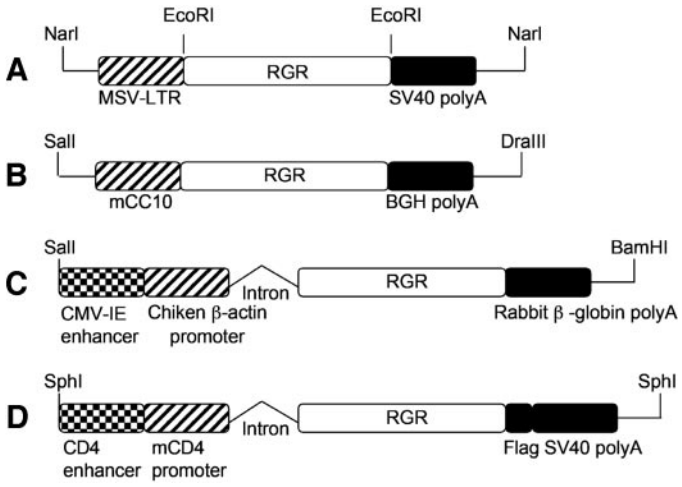

Fig. 1. Transgenic constructs generated with the Rgr oncogene. Four *Rgr* constructs were generated as described in Material and Methods. All of them include *Rgr* cDNA (*white boxes*) and differ in their promoter (*hatched* and *checkered boxes*) and poly(A) (*gray boxes*) sequences. Depending on the promoter sequence, the different constructs and mouse transgenic lines were termed MSV-RGR (*A*), mCC10-RGR (*B*), CMV-RGR (*C*), and CD4-RGR (*D*). In two of the cases (*C* and *D*), an intronic sequence was inserted between the promoter region and Rgr. Finally, Rgr was tagged with a Flag sequence (*black box*) in the CD4-RGR construct.

mouse lines as described previously (12, 13). The expression of Rgr was controlled by different promoters (Fig. 1): the Moloney murine sarcoma virus (MSV), which is expressed at significant levels in the brain (16), eye (16–18) and skeletal muscle (19) and at lower levels in the kidney, pancreas (16), and testis; the mCC10 promoter (mouse Clara Cell 10 KD protein), which is specific for the lung (20, 21), although it also drives a low level of expression in the uterus, ovaries, and epididymus of normal adults (21–23); and the CMV-IE enhancer plus the chicken β-actin promoter, which is ubiquitously expressed and starting from 4-cell stage (8).

Different results were obtained in the three cases in which the expression of the Rgr transgene was driven by nonlymphoid promoters. For the mCC10-RGR construct, after 2 years of study, gross morphological or behavioral abnormalities have not been detected in any of the transgenic mice. On the other hand, after three different experiments in which 244 fertilized eggs were injected with the CMV-RGR construct and a total of 50 mice were born, transgenic mice have not been obtained with this construct, which suggests that a high and ubiquitous expression of this oncogene at early embryonic stage could be lethal.

In the case of the MSV-RGR construct, a total of 11 transgenic lines were obtained that transmitted the transgene to their progeny. Five of these lines, with varying levels of expression in several tissues, were maintained as stable lines (L3, L21 L40, L43, and L58). Two of them, L21 and L43, were characterized and studied in more detail. Fig. 2*A* summarizes the RGR expression pattern as well as the major abnormalities found in the MSV-RGR lines. More than 95% of the mice bearing the transgene developed visible lens opacity at 3–6 weeks after birth. This opacity led to cataracts with swollen disoriented lens fibers and vacuolation of the lens (Fig. 2*B i* and *ii*). Associated with the cataracts, the presence of the oncogene elicited Harderian gland adenomas in all transgenic animals. MSV-RGR mice also exhibited inguinal hernias (Fig. 2*B iii*) that affected only males (90% of L43 males and 5% of L21 males), compromising male reproductive function and leading to sterility. More importantly, fibrosarcomas in the limbs and tail were found in 10% of the transgenic mice. Tumors were composed of atypical spindle-shaped cells that had a variable mitotic activity and appeared fibroblastic, arranged in intersecting fascicles, with collagenous stroma (Fig. 2*B iv*). These fibrosarcomas, which developed with a latency of 6–8 months, caused paralysis of the limbs in aged mice. These results indicated that Rgr acts as an oncogene and can produce tumors when overexpressed in transgenic mice.

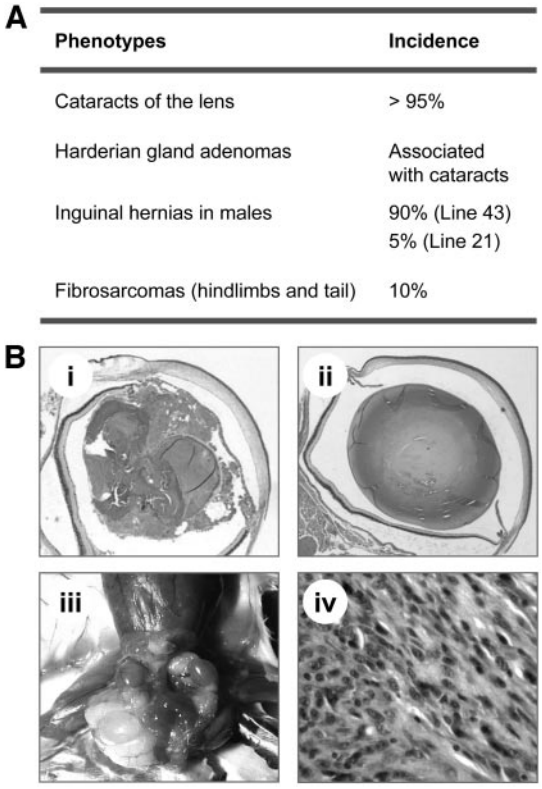

Fig. 2. Different phenotypes are observed in MSV-RGR transgenic mice. *A*, incidence of the different alterations detected in MSV-RGR transgenic mice. Note that with the exception of inguinal hernias, the incidence of the remaining alterations is the same in both lines. *B*, Pictures show different pathological alterations developed in transgenic mice. The histopathological analysis of MSV-RGR eyes showed lens cataract with disoriented lens fibers, vacuolation, and other malformations (*i*) compared with normal eye structure from a wild-type mouse (*ii*). In both *i* and *ii*, magnification is ×20. *iii*, surgical dissection showing an inguinal hernia developed in a male MSV-RGR transgenic mouse. *iv*, section of a fibrosarcoma from a MSV-RGR transgenic mouse, stained with hematoxylin and eosin; magnification, ×60.

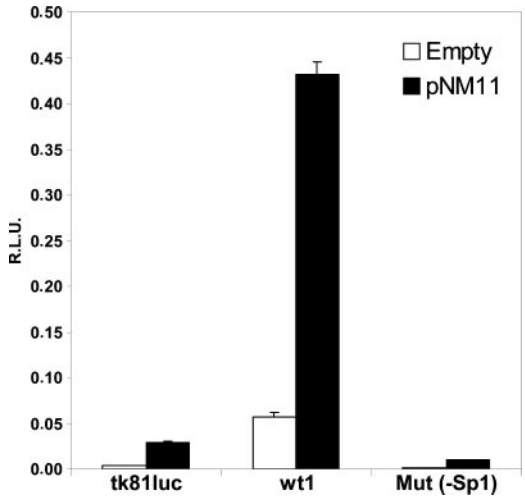

Fig. 3. Oncogenic Rgr induces $p15^{INK4b}$ expression through activation of its promoter. Representative experiment showing the induction of $p15^{INK4b}$ promoter activity by Rgr. NIH3T3 cells were cotransfected with Rgr and the pGL2b(−751/+160)-luc construct carrying a 751-bp sequence upstream of the $p15^{INK4b}$ ATG, the pGL2b(−35/+160)-luc construct carrying a sequence lacking Sp1 binding sites, or the tk81-luc construct as a negative control. Forty-eight hours after transfection, luciferase activity was measured as described in Material and Methods.

***Rgr* Cooperates with the Lack of *p15^{INK4b}* in the Tumoral Phenotype *In vivo*.** Tumoral processes are the result of an accumulation of alterations in genes regulating cellular homeostasis, such as oncogenes, tumor suppressor genes, apoptotic-regulating genes, and DNA repair genes. Because the MSV-RGR transgenic line showed a moderate tumor phenotype (10% of sarcomas with a 6- to 8-month latency period), we analyzed whether *Rgr*, as an oncogene, could cooperate *in vivo* with a tumor suppressor gene in tumor progression and development. Among all of the genes that have been associated with a tumor suppressor activity, we have previously demonstrated that the lack of one of them, *p15^{INK4b}*, cooperates with RGR in foci formation assays performed in mouse embryonic fibroblasts (10). Because this is the same collaboration type that we have found between Ras and $p15^{INK4b}$ (10), we studied whether or not Rgr also shares with Ras the mechanisms to activate the expression of $p15^{INK4b}$. NIH3T3 cells were cotransfected with Rgr and luciferase reporter plasmids containing either a wild-type form or different deletion mutants of the *p15^{INK4b}* promoter. Luciferase activity was measured 48 hours after transfections. As shown in Fig. 3, Rgr is indeed able to induce *p15^{INK4b}* expression in a fashion similar to that of Ras.

Given all these results suggesting that the cell cycle inhibitor $p15^{INK4b}$ is involved in tumor suppressor activity triggered by an

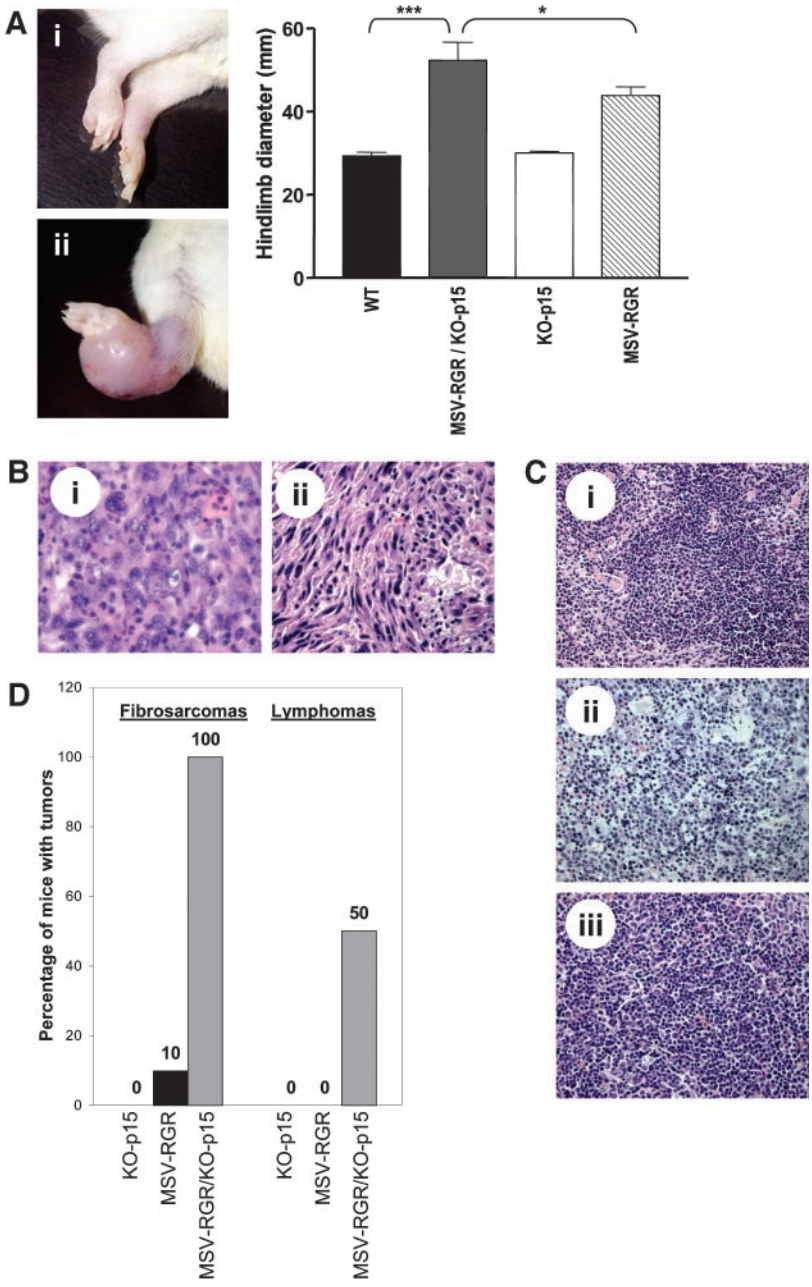

Fig. 4. Rgr cooperates with the lack of p15^{INK4b} in MSV-RGR-induced tumorigenesis. *A*, The severity of the fibrosarcomas induced by the MSV-RGR construct was substantially increased in a KO-p15^{INK4b} genetic background, as observed by the size of the tumors that developed in the limbs of MSV-RGR mice (*i*) compared with those in MSV-RGR/KO-p15^{INK4b} mice (*ii*). The *right bar graph* shows the quantification of ankle diameter in wild-type ($n = 7$), KO-p15^{INK4b} ($n = 9$), MSV-RGR ($n = 17$), and MSV-RGR/KO-p15^{INK4b} ($n = 20$) mice. *, $P < 0.05$; ***, $P < 0.0001$. *B*, sections of fibrosarcomas from the limb (*i*) and tail (*ii*) observed in MSV-RGR/KO-p15^{INK4b} mice. *C*, The normal cellular organization found in wild-type spleens (*i*) also was altered in MSV-RGR/KO-p15^{INK4b} mice. In 50% of the cases, extramedullary hematopoiesis (*ii*) was detected, whereas the rest of the cases were associated with lymphomas (*iii*). *D*, *Bar graph* shows the percentage of fibrosarcomas and lymphomas that are observed in KO-p15^{INK4b}, MSV-RGR, and MSV-RGR/KO-p15^{INK4b} mice. *B* and *C*, hematoxylin and eosin staining; magnification: ×60 (*B*) and ×40 (*C*).

inappropriate oncogenic Rgr activation, we decided to investigate the effect of Rgr oncogenic activation in a p15^{INK4b}-deficient background using a new transgenic/knockout mouse line that was generated by crossing the MSV-RGR and KO-p15^{INK4b} mouse lines (24). With this mouse model, we were able to demonstrate that lack of *p15^{INK4b}* could collaborate in the MSV-RGR-induced tumorigenesis inducing a more pronounced phenotype (Fig. 4). Indeed, the severity and incidence of the tumors induced by Rgr were substantially increased when the MSV-RGR transgenic mice were crossed with the KO-p15^{INK4b} mouse line. In fact, all of the MSV-RGR/KO-p15^{INK4b} mice developed fibrosarcomas in the limbs, tail, and/or ears, compared with only 10% of animals in the case of the MSV-RGR/WT-p15^{INK4b}. Furthermore, MSV-RGR/KO-p15^{INK4b} limb tumors were significantly larger than those found in the MSV-RGR/WT-p15^{INK4b} mice (Fig. 4*A*). Also, the latency of the fibrosarcomas diminished substantially from 24 to 32 weeks for the MSV-RGR mice in a wild-type p15^{INK4b} background to 3 to 6 weeks in a p15^{INK4b}-deficient one.

The histopathological analysis of the fibrosarcomas obtained from MSV-RGR/KO-p15^{INK4b} exhibited a more aggressive phenotype than those from MSV-RGR/WT-p15^{INK4b} mice, usually showing higher grade tumors with increased cellularity, mitotic activity, necrotic foci, and tumoral areas, with frequent multinucleated pleomorphic cells (undifferentiated pleomorphic sarcomas; Figs. 2*F* and 4*B*). In addition, all of the MSV-RGR/KO-p15^{INK4b} mice displayed lymphoid hyperplasia in the spleen (Fig. 4*C*). In 50% of these cases, this phenotype was a consequence of extramedullary hematopoiesis (foci of myeloid metaplasia in the red pulp composed of granulocytic cells, erythroblasts, and megakaryocytes in different stages of maturation), an abnormal phenotype that is also found in the p15^{INK4b}-null mice (24). More importantly, the remaining enlarged spleens were associated with lymphomas, a tumor type rarely found in KO-p15^{INK4b} mice (<1%; Ref. 24). These tumors were predominantly well-differentiated lymphomas, composed of small- to medium-sized cleaved centrocytes that usually expressed CD45R (B220) and IgM (data not shown),

whereas infiltration of the white and red pulp was variable. Thus, the concurrent presence of both genetic alterations, expression of oncogenic *Rgr* together with the loss of *p15^{INK4b}*, has a synergistic effect in the tumoral phenotype (Fig. 4*D*).

To demonstrate the specificity of p15^{INK4b} in cooperation with Rgr in this mouse transgenic model, we studied the expression of other tumor suppressor genes by immunohistochemistry. Specifically, we chose the following for this analysis: p16^{INK4a} (like p15^{INK4b}, an INK4 family member that has been found to be down-regulated in many tumor types); p21^{kip1} (another RB function inhibitor; in this case, a member of the CIP/KIP family); and, finally, p53, the key molecule of the other critical pathway most frequently mutated in tumorigenesis. Interestingly, none of these three genes was down-regulated in any of the seven tumors analyzed (Fig. 5). Moreover, we did not find overexpression of p53, suggesting that this gene is not mutated in any of the analyzed tumors. Therefore, these results appear to indicate a specific role of the constitutive lack of *p15^{INK4b}* in RGR-induced tumorigenesis.

CD4-RGR Transgenic Mice: A Key Role of *Rgr* in T-Cell Lymphoma Development and Progression. Mutations in the *Rgr* human orthologue, *hrgr*, have been associated with human T-cell malignancies (7). In contrast, MSV-RGR transgenic mice expressing low levels of Rgr in lymphoid tissues (data not shown) are prone to splenic lymphomas in a *p15^{INK4b}*-deficient background (Fig. 4*C* and *D*). To further analyze *in vivo* the role of *Rgr* in lymphomagenesis, new transgenic mouse lines were generated in which *Rgr* expression was under the control of the murine CD4 minimal promoter (lacking the CD4 silencer region) and the CD4 enhancer (Fig. 1*D*) to drive the expression in CD4- and CD8-positive T cells (both single and double positive; Ref. 10). Among the 16 founders obtained from microinjection of the CD4-RGR-Flag transgene, three independent CD4-RGR transgenic lines (lines 19, 37, and 42), were expanded and studied. The thymocytes of the animals in all three lines exhibited Rgr expression (data not shown). As shown in Fig. 6*A*, many animals (83% in L19, 38% in L37, and 68% in L42) carrying the CD4-RGR construct developed thymic lymphomas. In fact, the progression of this tumor was the cause of death in all cases. Lines 19 and 42 showed similar thymic lymphoma incidence curves in the first year of life (median latency of 22 and 20 weeks and tumor-free ratios of 6.7% and 13.2%, respectively). A weaker phenotype was displayed by line 37 (median latency of 35 weeks and tumor-free ratio at 1 year of age of 37%). The neoplasms caused complete effacement of the normal thymic architecture and frequently infiltrated adjacent soft tissues and lung (Fig. 6*B*).

To further characterize the *in vivo* oncogenic effect of Rgr expression in mouse thymocytes, the expression profile of different T-cell surface markers was determined. A series of thymic lymphomas showed that the majority of these tumors were, CD4^{+}, CD8$^{+/-}$, and CD25^{+} (Fig. 6*C*). To characterize the putative effects resulting from the expression of Rgr in preneoplastic thymocytes, the morphological and phenotypic features of thymocyte populations in line 42 and in the less clinically aggressive line 37 were studied. Microscopic evaluation demonstrated a normal thymic architecture and no significant differences between the transgenic mice and normal control littermates (data not shown). However, a reproducible but minimal reduction in the total number of thymocytes was observed in lines 37 and 42 (Fig. 7), although this decrease in the number of cells of the CD4-RGR thymi was not statistically significant. Moreover, when 6-week-old mice were used to isolate and study the frequency of different T-cell subpopulations by flow cytometric analysis, significant differences were detected between CD4-RGR and wild-type thymocytes (Fig. 7). These differences were more pronounced in the case of the CD4-RGR mice line with shorter latency and higher incidence of thymic lymphomas (line 42). Indeed, a significant reduction was found in the thymocyte subpopulation expressing high levels of T-cell receptor (CD3high) and the single-positive CD4 and CD8 thymocytes, together with an increase in the number of CD4/CD8 double-positive cells. No significant differences were found for the percentages of CD4/CD8 double-negative thymocytes. Higher levels of CD25-, CD44-, and CD69-positive thymocytes among CD4-RGR line 42 mice were also detected. However, only the percentages of CD25- and CD69-positive thymocytes were significantly altered in the CD4-RGR line with longer latency and lower incidence (line 37).

All these results indicated that Rgr expression in the thymocytes of immature mice induced a severe alteration on the patterns of thymocyte development and maturation consisting of a substantial increase in the number of activated and undifferentiated cells. These alterations preceded the development of lymphomas.

Finally, because lack of *p15^{INK4b}* in mice carrying a MSV-RGR construct induces a more pronounced malignant phenotype, including the onset of spleen lymphomas, we investigated whether or not p15^{INK4b} down-regulation also plays a critical role in CD4-RGR-induced lymphomagenesis. The expression levels of *p15^{INK4b}* mRNA were determined in a set of CD4-RGR thymic lymphomas by real-time RT-PCR. As shown in Fig. 8, 50% of the tumors analyzed showed a significant down-regulation of p15^{INK4b} expression. Also, it is interesting to note that in the other 50% of the samples, p15^{INK4b} was overexpressed, which confirmed our *in vitro* results on the capacity of Rgr to induce p15^{INK4b} expression (Fig. 3). These results support the functional interplay between Rgr and p15^{INK4b} and suggest that oncogenic activation of *Rgr* and lack of *p15^{INK4b}* expression cooperate in different tumor types.

A

Tumors	p53	p21	p16
6817T	+	++	+++
6609T	+	++	+
6595TA	+	+	+
6639F	+	+	+
6626MST	+	+	+
6735T	+	++	+
6866TA	++	+++	+++

B

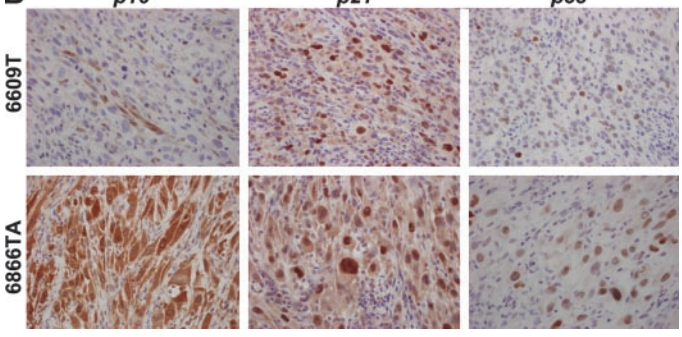

Fig. 5. Specific role of the lack of p15^{INK4b} in MSV-RGR/KO-p15^{INK4b} fibrosarcomas. *A. Table* shows p21, p16, and p53 protein expression levels detected by immunohistochemistry in seven MSV-RGR/KO-p15^{INK4b} fibrosarcomas. Protein expression: +, 5–50% positive cells; ++, >50% positive cells; and, +++, >50% positive cells with high levels of expression per cell. *B.* Representative pictures show the expression of p16, p21, and p53 in two different MSV-RGR/KO-p15^{INK4b} fibrosarcomas. Sample 6609T shows normal expression of both p16 and p53 and moderated overexpression of p21. Sample 6866TA shows overexpression of the three analyzed proteins.

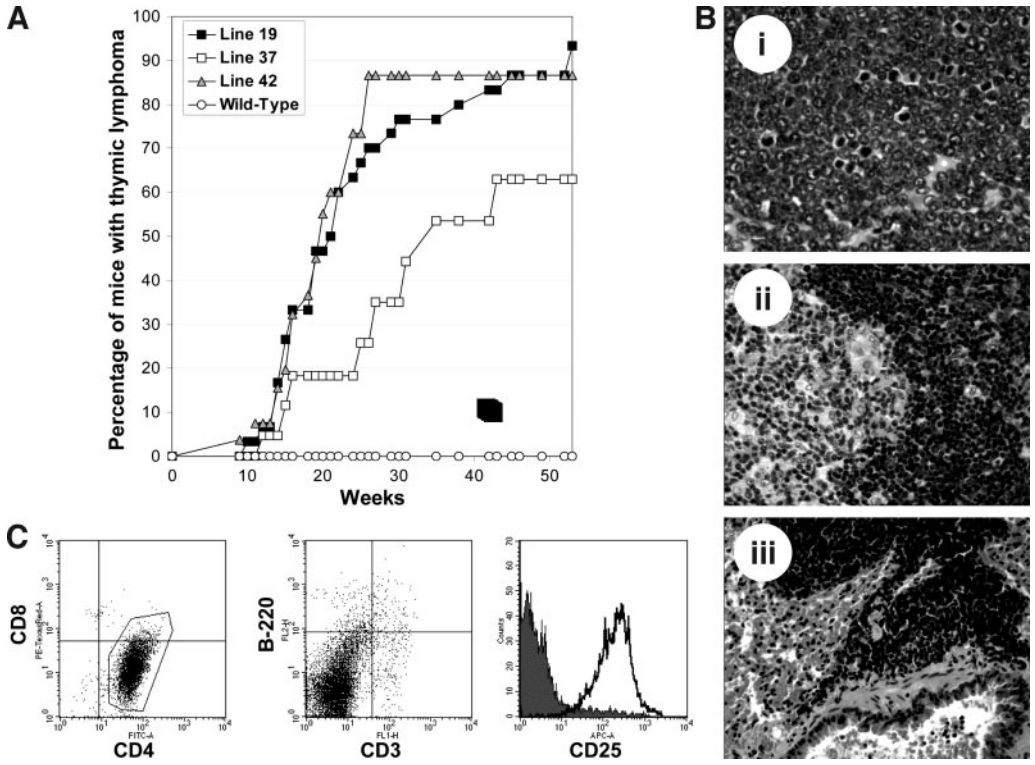

Fig. 6. CD4-RGR transgenic mice develop thymic lymphomas. *A*, thymic lymphoma incidence in the three CD4-RGR lines studied in this work. The number of mice used per line was as follows: 30 (line 19), 23 (line 42), 27 (line 42), and 30 (wild-type). *B*, representative sections of (*i*) a malignant thymic lymphoma in line 19 showing a monomorphic population of large, noncleaved lymphoid cells, with high mitotic index; (*ii*) a normal thymus from a wild-type mouse of the same age; and (*iii*) an infiltration by a CD4-RGR lymphoma in the lung showing patchy small infiltrates by monomorphic large- to medium-sized lymphocytes. Magnification: ×630 (*i* and *ii*) and ×400X (*iii*). *C*, typical phenotype of CD4-RGR thymic lymphomas. Tumor cells obtained from neoplastic thymus were stained with the indicated antibodies and analyzed by fluorescence-activated cell sorting.

DISCUSSION

Rgr Is the First Ral Guanine Nucleotide Exchange Factor Family Member with Transforming Activity *In vivo*. Rgr is a GEF protein that was isolated in our laboratory by its ability to produce tumors in nude mice (1). The role of GEFs in activating pathways mediated by small GTPases indicates that they could play a pathogenic role in some tumors in which these pathways are abnormally induced. There are several GEFs, such as dbl, vav, and CALDAG-GEF1, previously identified as oncogenes that have been found to be mutated or rearranged in human (25, 26) and animal malignancies (27). However, it is interesting to note that among all of the constitutively activated variants of the RalGEFs, only Rgr is transforming by itself in mouse cells (3). The remaining GEFs, although they are not transforming, cooperate with activated Raf in focus formation processes (2, 28). Unlike in mouse cells, the RalGEF pathway has been reported to be important for Ras-mediated transformation in human cells (7, 29). *In vivo* studies have shown previously that activation of RalGEF is sufficient to initiate an invasive phenotype in nude mice (30). The present study demonstrates that Rgr displays tumorigenic properties in a mouse transgenic model because it is able to produce tumors in some of the tissues in which it is overexpressed.

The only known substrates for the RalGEFs are the monomeric G-proteins RalA and RalB. However, oncogenic potential has not been shown for activated Ral proteins alone, although they facilitate Ras transformation, participate in cell motility, and are required for metastatic evolution of Ras-transformed cells and for Ras-induced stimulation of cyclin D1 expression (28–34). Interestingly, Rgr also is able to activate Ras (3), which could explain its potency as an oncogene and its ability to transform cells and promote tumor formation in transgenic mice.

Rgr and p15^{INK4b} Cooperate in the Development and Progression of Different Tumor Types. Tumor development and progression are associated with multiple genetic lesions. Although it is not known which altered genes are cooperating with Rgr in tumorigenic processes, one of the candidates is the tumor suppressor gene *p15^{INK4b}*. In a previous study, p15^{INK4b} produced G_1 arrest in Ras-transformed cells and decreased the tumorigenic potential of Ras and Rgr in focus formation assays in mouse fibroblasts (4). In addition, we have shown that, like oncogenic Ras, activation of oncogenic Rgr triggers p15^{INK4b} expression (Fig. 3), which could be part of a more general antioncogenic response. Therefore, similar to oncogenic Ras, Rgr and p15^{INK4b} interact *in vitro* in such a way that alteration of both genes cooperates in the malignant phenotype. These results are consistent with the fact that although Rgr is able to activate both Ral and Ras, its transforming activity is dependent on Ras and less so on Ral (3).

The role of p15^{INK4b} in tumorigenesis is not well defined. Although the *INK4b* locus is often deleted in human tumors, its loss is concomitant with that of the *INK4a/ARF* locus (35). In some cases, however, deletion of *p15^{INK4b}* occurs independently of *p16^{INK4a}* status (36, 37). More recently, it has been described that a small fraction of the KO-p15^{INK4b} mice develop different types of tumors, mainly sarcomas (24). The high incidence of tumors observed in the double-mutant MSV-Rgr/KO-p15^{INK4b} mice (100%), compared with that obtained in both the MSV-Rgr (10%) and KO-p15^{INK4b} (8.2%) mouse lines, clearly demonstrates the synergistic cooperation between p15^{INK4b} and the Rgr oncogene *in vivo*.

It has been described that inhibition of p15^{INK4b} expression appears to be a common event in human lymphoid tumors and mouse T-cell lymphomas (37–41). Here, the important role of p15^{INK4b} in lymphomagenesis is confirmed. Furthermore, the results indicate that the role of p15^{INK4b} in tumorigenesis is dependent on the concurrent oncogenic activation of various components of the Ras pathway. Indeed, splenic lymphomas are found in 50% of MSV-RGR/KO-p15^{INK4b} mice, whereas this tumor type is found in <1% of KO-p15^{INK4b} mice, which only show extramedullary hematopoiesis. In accordance with these observations, similar results have been obtained when crossing transgenic mice expressing an N-Ras oncogenic variant

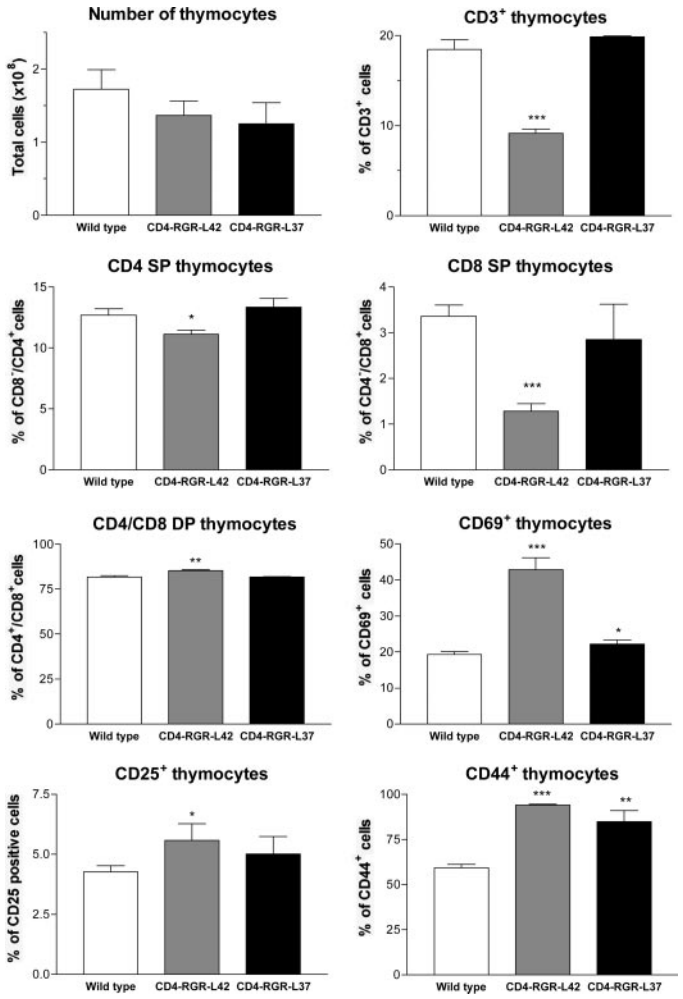

Fig. 7. Characterization of CD4-RGR preneoplasic thymi. Phenotypic features of wild-type and CD4-RGR thymi. Thymocytes were isolated from a total of twelve 6-week-old mice (6 wild-type and 6 CD4-RGR mice). Half of the CD4-RGR mice came from line 37 (*L37*), whereas the remaining mice corresponded to the most aggressive of the lines (*L42*). *Bar graphs* show the total number of cells (*top left panel*) or percentages of $CD3^+$high, $CD69^+$, $CD4^+/CD25^+$, $CD8^+/CD25^+$, and $CD44^+$ thymocytes (*remaining panels*) detected by flow cytometric analysis. Wild-type and CD4-RGR populations were compared using unpaired *t* tests. *, $P < 0.05$; **, $P < 0.001$; ***, $P < 0.0001$.

with $p15^{INK4b}$-KO mice.[4] Finally, the results derived from the study of the CD4-RGR tumors constitute not only additional evidence in favor of the role of alterations in both genes in lymphomagenesis but also a new and significant observation about the collaboration of the two of them in this kind of tumor.

The *INK4b* gene and the closely related gene, *INK4a*, are located at the same chromosomal region in both the human and mouse genome, a hot spot for cancer-associated deletions (37, 42). Although the inactivation of $p16^{INK4a}$ has been clearly associated with cancer development and progression (43), the role of $p15^{INK4b}$ as a tumor suppressor gene is still controversial. Therefore, our data constitute new and strong evidence in favor of the critical role of $p15^{INK4b}$ inactivation in the development and progression of some tumor types.

Critical Role of Rgr Oncogenic Activation in T-Cell Tumorigenesis. An important conclusion derived from this work is the role of Rgr in lymphomagenesis. As it has been described above, MSV-RGR mice lacking $p15^{INK4b}$ showed a remarkable increase in splenic B-cell lymphoma incidence. These results are remarkable, considering that Rgr expression in the spleen of these transgenic mice is modest (data not shown). CD4-RGR transgenic mice provided additional confirmation of the role of Rgr in lymphomagenesis. The expression of Rgr under control of the CD4 promoter induces thymic lymphomagenesis (Fig. 6). The fact that NrasT transgenic mice develop thymic lymphomas (44) is consistent with our previous results *in vitro*, in which the transforming activity of Rgr is mediated predominantly by Ras.

The study of preneoplastic CD4-RGR thymi produced important insights regarding the Rgr-induced alterations in T cells. In the CD4-RGR transgenic line with higher incidence of tumors and shorter latency, 6-week-old mice showed a significantly altered pattern of their thymocyte subpopulations (Fig. 7). The reduction in the number of $CD3^{+high}$, $CD4^+CD8^-$, and $CD4^-CD8^+$ cells indicated an increase in the number of undifferentiated thymocytes. Moreover, these cells became more activated, as demonstrated by the levels of expression of specific activation markers (CD25 and CD69). The most interesting results derived from the analysis of the CD44 marker. CD44 is a multistructural and multifunctional cell surface molecule that has been involved in many cellular functions from cell proliferation to cell migration and angiogenesis. In this case, both CD4-RGR transgenic mice lines (lines 42 and 37) showed a similar and substantial increase in the number of $CD44^+$ thymocytes. Interestingly, CD44 has been associated with cancer (45), and it has been proposed as a good candidate to predict prognosis in patients with lymphoma (46). Our data suggest that CD44 overexpression could be a candidate marker for early detection of Rgr-induced lymphomagenesis.

Recently, the human orthologue of *Rgr*, *hrgr*, has been associated with human T-cell malignancies (7). Similar to rabbit Rgr, which was found as one of the components of a fusion protein isolated from a rabbit squamous cell carcinoma, truncation of *hrgr* confers transforming properties to its cDNA. DNA rearrangements, which are frequent events in T-cell lymphomagenesis (47), could have resulted in *hrgr* truncation. Indeed, a DNA rearrangement has been found within the *hrgr* gene in a human anaplastic large cell lymphoma cell line (DHL; Ref. 7). It is interesting to point out that chromosomal translocations frequently have been associated with sarcomagenesis (48), and in many cases, these

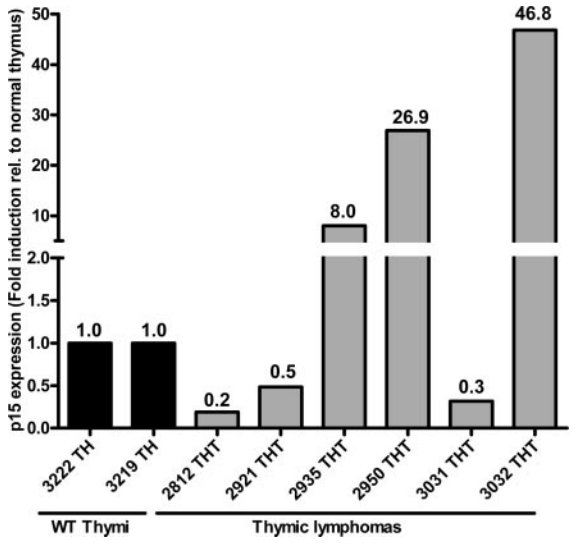

Fig. 8. Expression of $p15^{INK4b}$ in CD4-RGR thymic lymphomas. Total RNA was isolated from two wild-type (*WT*) thymi and six CD4-RGR thymic lymphomas. Real-time RT-PCR was performed in triplicate as described in Material and Methods to determine mRNA expression levels of $p15^{INK4b}$ in all of the samples. Normal and lymphoma values were calculated relative to one of the wild-type samples (*3222 TH*).

[4] I. Pérez de Castro, M. Malumbres, M. Benet, M. Jiménez, J. F. García, M. Barbacid, A. Pellicer. Effect of $p15^{INK4b}$ deficiency on N-ras mediated oncogenesis, manuscript in preparation.

genetic translocations affect a chromosomal region close to the one in which hrgr is located (22q11.2). Therefore, there is a need for additional studies on the role of hrgr in human sarcomagenesis. According to our preliminary results, DNA rearrangements involving Rgr provoke changes in its levels of expression. In normal cells and tissues, the levels of expression of both Rgr and hrgr are low, whereas in transformed cells and tumor samples, a significant level of expression of these genes is detected (3, 7). In this work, overexpression of oncogenic Rgr is sufficient to induce the development of fibrosarcomas and lymphomas. Thus, our previous *in vitro* model is corroborated, in which a mutation affecting the regulation of gene expression, which increases its expression from negligible levels, is the basis for Rgr acting as an oncogene (6). However, neoplastic alterations have not been detected in some of the tissues in which Rgr has been overexpressed. For example, the MSV-RGR mice express substantial levels of Rgr in liver, brain, and kidney (data not shown), and pathological alterations have not been detected in those tissues after analysis of these transgenic mice at age $>$ 2 years. Therefore, these results suggest that the Rgr-induced transforming phenotype is dependent not only on the expression levels of this gene but also on certain tissue-specific factors. These still uncharacterized elements might be the reason for oncogenic Rgr involvement in lymphomagenesis and, to a lesser extent, in the development of fibrosarcomas.

Taken together, these results reinforce the role of *Rgr* as an oncogene in different tumor types. In some of the tumors (fibrosarcomas), Rgr-induced tumorigenesis is substantially potentiated by the effect of other genetic alterations, such as a constitutive lack of $p15^{INK4b}$ expression. However, in other cases (lymphomas), expression of Rgr in T cells induced a severe alteration of thymocyte differentiation and strengthens the notion that Rgr plays an important role in lymphomagenesis. Therefore, the high incidence of lymphomas and fibrosarcomas in the transgenic lines and the fact that hrgr also is associated with human lymphomas support this as a model to study sarcomagenesis and lymphomagenesis.

ACKNOWLEDGMENTS

We are especially indebted to E. Latres and M. Barbacid for providing us with the $p15^{INK4b}$-deficient mice. We also want to thank John Hirst for his help in flow cytometric analyses and Laura Martello-Roonie for critical reading of the manuscript.

REFERENCES

1. D'Adamo DR, Novick S, Kahn JM, Leonardi P, Pellicer A. rsc: a novel oncogene with structural and functional homology with the gene family of exchange factors for Ral. Oncogene 1997;14:1295–305.
2. White MA, Vale T, Camonis JH, Schaefer E, Wigler MH. A role for the Ral guanine nucleotide dissociation stimulator in mediating Ras-induced transformation. J Biol Chem 1996;271:16439–42.
3. Hernandez-Munoz I, Malumbres M, Leonardi P, Pellicer A. The Rgr oncogene (homologous to RalGDS) induces transformation and gene expression by activating Ras, Ral and Rho mediated pathways. Oncogene 2000;19:2745–57.
4. Malumbres M, Perez De Castro I, Hernandez MI, et al. Cellular response to oncogenic ras involves induction of the Cdk4 and Cdk6 inhibitor $p15^{INK4b}$. Mol Cell Biol 2000;20:2915–25.
5. Perez de Castro IP, Malumbres M, Santos J, Pellicer A, Fernandez-Piqueras J. Cooperative alterations of Rb pathway regulators in mouse primary T cell lymphomas. Carcinogenesis (Lond) 1999;20:1675–82.
6. Hernandez-Munoz I, Benet M, Calero M, et al. rgr oncogene: activation by elimination of translational controls and mislocalization. Cancer Res 2003;63: 4188–95.
7. Leonardi P, Kassin E, Hernandez-Munoz I, et al. Human rgr: transforming activity and alteration in T-cell malignancies. Oncogene 2002;21:5108–16.
8. Okabe M, Ikawa M, Kominami K, Nakanishi T, Nishimune Y. "Green mice" as a source of ubiquitous green cells. FEBS Lett 1997;407:313–9.
9. Martin-Zanca D, Oskam R, Mitra G, Copeland T, Barbacid M. Molecular and biochemical characterization of the human trk proto-oncogene. Mol Cell Biol 1989; 9:24–33.
10. Sawada S, Scarborough JD, Killeen N, Littman DR. A lineage-specific transcriptional silencer regulates CD4 gene expression during T lymphocyte development. Cell 1994;77:917–29.
11. Wigler M, Pellicer A, Silverstein S, Axel R. Biochemical transfer of single-copy eucaryotic genes using total cellular DNA as donor. Cell 1978;14:725–31.
12. Gordon JW, Scangos GA, Plotkin DJ, Barbosa JA, Ruddle FH. Genetic transformation of mouse embryos by microinjection of purified DNA. Proc Natl Acad Sci USA 1980;77:7380–4.
13. Gordon JW, Ruddle FH. Gene transfer into mouse embryos: production of transgenic mice by pronuclear injection. Methods Enzymol 1983;101:411–33.
14. Taketo M, Schroeder AC, Mobraaten LE, et al. FVB/N: an inbred mouse strain preferable for transgenic analyses. Proc Natl Acad Sci USA 1991;88:2065–9.
15. Malumbres M, Mangues R, Ferrer N, Lu S, Pellicer A. Isolation of high molecular weight DNA for reliable genotyping of transgenic mice. Biotechniques 1997;22: 1114–9.
16. Theuring F, Gotz W, Balling R, et al. Tumorigenesis and eye abnormalities in transgenic mice expressing MSV-SV40 large T-antigen. Oncogene 1990;5:225–32.
17. Khillan JS, Oskarsson MK, Propst F, et al. Defects in lens fiber differentiation are linked to c-mos overexpression in transgenic mice. Genes Dev 1987;1:1327–35.
18. Gotz W, Theuring F, Favor J, Herken R. Eye pathology in transgenic mice carrying a MSV-SV 40 large T-construct. Exp Eye Res 1991;52:41–9.
19. Sutrave P, Copeland TD, Showalter SD, Hughes SH. Characterization of chicken c-ski oncogene products expressed by retrovirus vectors. Mol Cell Biol 1990;10: 3137–44.
20. DeMayo FJ, Damak S, Hansen TN, Bullock DW. Expression and regulation of the rabbit uteroglobin gene in transgenic mice. Mol Endocrinol 1991;5:311–8.
21. Sandmoller A, Voss AK, Hahn J, et al. Cell-specific, developmentally and hormonally regulated expression of the rabbit uteroglobin transgene and the endogenous mouse uteroglobin gene in transgenic mice. Mech Dev 1991;34:57–67.
22. Gomez Lahoz E, Lopez de Haro MS, Esponda P, Nieto A. Tissue-specific and hormonally regulated expression of the puromycin N-acetyltransferase-encoding gene under control of the rabbit uteroglobin promoter in transgenic mice. Gene (Amst) 1992;117:255–8.
23. Margraf LR, Finegold MJ, Stanley LA, et al. Cloning and tissue-specific expression of the cDNA for the mouse Clara cell 10 kD protein: comparison of endogenous expression to rabbit uteroglobin promoter-driven transgene expression. Am J Respir Cell Mol Biol 1993;9:231–8.
24. Latres E, Malumbres M, Sotillo R, et al. Limited overlapping roles of $P15^{INK4b}$ and $P18^{INK4c}$ cell cycle inhibitors in proliferation and tumorigenesis. EMBO J 2000;19: 3496–506.
25. Zhu K, Debreceni B, Bi F, Zheng Y. Oligomerization of DH domain is essential for Dbl-induced transformation. Mol Cell Biol 2001;21:425–37.
26. Katzav S, Martin-Zanca D, Barbacid M. vav, a novel human oncogene derived from a locus ubiquitously expressed in hematopoietic cells. EMBO J 1989;8:2283–90.
27. Dupuy AJ, Morgan K, von Lintig FC, et al. Activation of the Rap1 guanine nucleotide exchange gene, CalDAG-GEF I, in BXH-2 murine myeloid leukemia. J Biol Chem 2001;276:11804–11.
28. Urano T, Emkey R, Feig LA. Ral-GTPases mediate a distinct downstream signaling pathway from Ras that facilitates cellular transformation. EMBO J 1996;15:810–6.
29. Hamad NM, Elconin JH, Karnoub AE, et al. Distinct requirements for Ras oncogenesis in human versus mouse cells. Genes Dev 2002;16:2045–57.
30. Ward Y, Wang W, Woodhouse E, et al. Signal pathways which promote invasion and metastasis: critical and distinct contributions of extracellular signal-regulated kinase and Ral-specific guanine exchange factor pathways. Mol Cell Biol 2001; 21:5958–69.
31. Gildea JJ, Harding MA, Seraj MJ, Gulding KM, Theodorescu D. The role of Ral A in epidermal growth factor receptor-regulated cell motility. Cancer Res 2002;62: 982–5.
32. Henry DO, Moskalenko SA, Kaur KJ, et al. Ral GTPases contribute to regulation of cyclin D1 through activation of NF-kappaB. Mol Cell Biol 2000;20:8084–92.
33. Lee T, Feig L, Montell DJ. Two distinct roles for Ras in a developmentally regulated cell migration. Development (Camb) 1996;122:409–18.
34. Suzuki J, Yamazaki Y, Li G, Kaziro Y, Koide H. Involvement of Ras and Ral in chemotactic migration of skeletal myoblasts. Mol Cell Biol 2000;20:4658–65. Erratum in: Mol Cell Biol 2000;20:7049.
35. Stone S, Dayananth P, Jiang P, et al. Genomic structure, expression and mutational analysis of the P15 (MTS2) gene. Oncogene 1995;11:987–91.
36. Glendening JM, Flores JF, Walker GJ, et al. Homozygous loss of the p15INK4B gene (and not the p16INK4 gene) during tumor progression in a sporadic melanoma patient. Cancer Res 1995;55:5531–5.
37. Malumbres M, Perez de Castro I, Santos J, et al. Inactivation of the cyclin-dependent kinase inhibitor p15INK4b by deletion and de novo methylation with independence of p16INK4a alterations in murine primary T-cell lymphomas. Oncogene 1997;14: 1361–70.
38. Herman JG, Jen J, Merlo A, Baylin SB. Hypermethylation-associated inactivation indicates a tumor suppressor role for p15INK4B. Cancer Res 1996;56:722–7.
39. Herman JG, Civin CI, Issa JP, et al. Distinct patterns of inactivation of p15INK4B and p16INK4A characterize the major types of hematological malignancies. Cancer Res 1997;57:837–41.

40. Batova A, Diccianni MB, Yu JC, et al. Frequent and selective methylation of p15 and deletion of both p15 and p16 in T-cell acute lymphoblastic leukemia. Cancer Res 1997;57:832–6.
41. Malumbres M, Perez de Castro I, Santos J, Fernandez Piqueras J, Pellicer A. Hypermethylation of the cell cycle inhibitor p15INK4b 3′-untranslated region interferes with its transcriptional regulation in primary lymphomas. Oncogene 1999;18: 385–96.
42. Kamb A, Shattuck-Eidens D, Eeles R, et al. Analysis of the p16 gene (CDKN2) as a candidate for the chromosome 9p melanoma susceptibility locus. Nat Genet 1994;8: 23–6.
43. Ruas M, Peters G. The p16INK4a/CDKN2A tumor suppressor and its relatives. Biochim Biophys Acta 1998;1378:F115–77.
44. Mangues R, Symmans WF, Lu S, Schwartz S, Pellicer A. Activated N-ras oncogene and N-ras proto-oncogene act through the same pathway for in vivo tumorigenesis. Oncogene 1996;13:1053–63.
45. Naor D, Nedvetzki S, Golan I, Melnik L, Faitelson Y. CD44 in cancer. Crit Rev Clin Lab Sci 2002;39:527–79.
46. Pals ST, Drillenburg P. CD44 expression predicts disease outcome in localized large B cell lymphoma. Blood 2000;95:1900–10.
47. Downing JR, Shurtleff SA, Zielenska M, et al. Molecular detection of the (2;5) translocation of non-Hodgkin's lymphoma by reverse transcriptase-polymerase chain reaction. Blood 1995;85:3416–22.
48. Helman LJ, Meltzer P. Mechanisms of sarcoma development. Nat Rev Cancer 2003;3:685–94.